Electroluminescence from monolayer ZnO nanoparticles using dry coating technique

Chun-Yu Lee,[1] Yuen-Yung Hui,[1] Wei-Fang Su,[2] and Ching-Fuh Lin[1,3,a]

[1]*Graduate Institute of Photonics and Optoelectronics, National Taiwan University, Taipei 10617, Taiwan*
[2]*Graduate Institute of Materials Science and Engineering and Department of Materials Science and Engineering, National Taiwan University, Taipei 10617, Taiwan*
[3]*Graduate Institute of Electronics Engineering and Department of Electrical Engineering, National Taiwan University, Taipei 10617, Taiwan*

We report ultraviolet electroluminescence from ZnO nanoparticle-based devices prepared by the dry-coating technique. With dry-coating process, the structure of the ZnO nanoparticle monolayer (90 nm) in the device can be easily achieved. The method reduces the density of pinhole defects in the ZnO nanoparticles. The confirmation for dry coating is investigated using field-emission scanning electron microscopy. The devices show the ZnO band-gap emission peak at 380 nm and the background emission from the interface between the host matrix and Aluminum tris-8-hydroxyquinoline. The origins of the ZnO band-gap emission and background emission are also discussed. © *2008 American Institute of Physics*. [DOI: 10.1063/1.2952283]

Zinc oxide (ZnO) is a promising semiconductor with a wide direct band-gap of 3.37 eV. Due to its large exciton binding energy (60 meV), the excitons in ZnO are thermally stable at room temperature. It has been regarded as one of the most promising candidates for the next generation of ultraviolet (UV)-blue light-emitting diodes (LEDs) and lasing devices operating at high temperatures and in harsh environments. A few studies have been reported on the development of heterojunction LEDs using ZnO thin film,[1–7] ZnO nanowires,[8–14] or ZnO nanoparticles.[15,16] In the past, we have reported the use of phase-segregation technique to fabricate the ZnO nanoparticle electroluminescent (EL) devices.[16] With phase segregation, the ZnO nanoparticles and organic material will form a heterostructure. This method can improve the probability that electrons and holes recombine in the ZnO nanoparticles to enhance the band-gap emission. However, it is not easy to achieve the phase segregation. In addition, the thickness of ZnO nanoparticles is very difficult to control. Here we report an approach, dry-coating method, to fabricate ZnO EL devices with heterostructure. The ZnO monolayer can be easily achieved by dry coating. Unlike the phase segregation, which requires a particular type of hole-transporting material and special conditions of solvents, the dry-coating method is applicable to several hole-transporting materials. The method has the prominent advantage of making the cost of ZnO EL devices less expensive.

In this work, we prepare three types of ZnO EL devices formed with a host polymer, ZnO nanoparticle monolayer, and an electron transporting layer. The following host matrix materials dissolving in chloroform with different concentration are chosen respectively: 0.7 wt % poly(fluorene) (PF), 1 wt % poly(*N*-vinylcarbazole) (PVK), and 0.7 wt % poly(3-hexylthiophene) (P3HT). For the electron transporting layer we employed small-molecular aluminum tris-8-hydroxyquinoline (Alq3). The ZnO nanoparticles were purchased from Aldrich. The diameter of the ZnO nanoparticles

is 90 nm. The procedure of device fabrication is as follows. First, we clean the indium tin oxide (ITO) glass by deionized water, acetone, and isopropyl alcohol sequentially. Then the host matrixes are spin coated on ITO glass respectively. In order to get the optimized film-forming property, the different host matrixes have the different thickness by different spin-coating condition (PF: 200 nm, PVK: 900 nm, and P3HT: 110 nm). These samples are baked at 170 °C (device I), 170 °C (device II), and 120 °C (device III) for 2 h individually. Then we deposit the ZnO nanoparticles on each host matrix by dry coating under the temperature of 85 °C and subsequently annealed at 120 °C for 2 h to improve the contact between the ZnO nanoparticles and the host matrix. Then the solution containing the 0.5 wt % Alq3 is spun on top of the ZnO nanoparticles and subsequently annealed at 60 °C for 2 h to remove the solvent. Afterward, 2000 Å of aluminum (Al) was deposited onto the electron transporting layer using thermal evaporation under a vacuum of 3×10^{-6} torr. The emitting area is 0.7×0.3 cm^2. The device structure is ITO/host matrix/ZnO nanoparticles (monolayer)/Alq3/Al. The schematic of the device structure is shown in Fig. 1(a).

In the past, the organic/inorganic EL devices are mainly fabricated by spin coating.[14–16] The organic/inorganic nanocomposites are formed through dispersion of inorganic nanoparticles within the polymer matrix.[14–16] However, the hybrid structure is a disadvantage for carrier recombination in nanoparticles due to the high density of pinhole defects
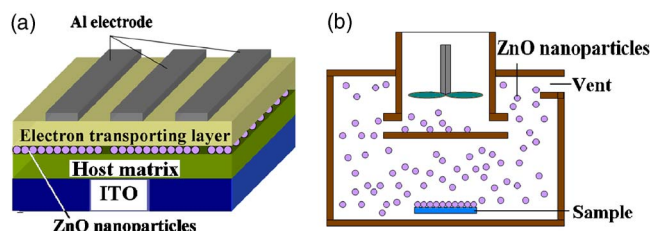

FIG. 1. (Color online) (a) Cross-sectional schematic of the ZnO EL device structure. (b) The schematic of the dry-coating machine.

[a]Author to whom correspondence should be addressed. Tel.: 886-2-3366 3540. FAX: 886-2-2364 2603. Electronic mail: cflin@cc.ee.ntu.edu.tw.
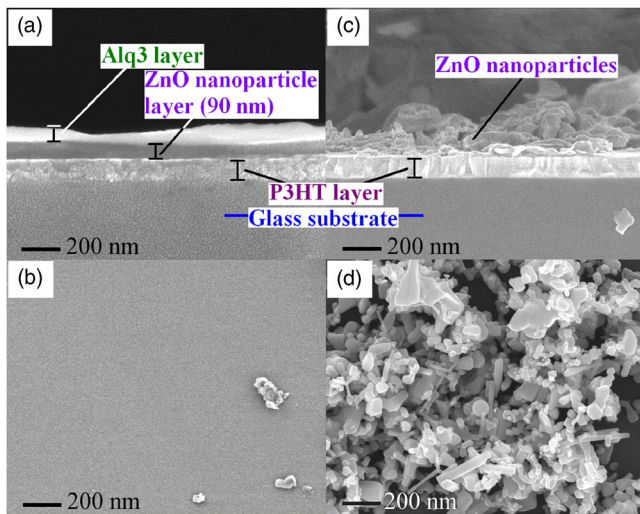
FIG. 2. (Color online) FESEM images of the ZnO nanoparticle layer (a) after spin Alq3 (cross-sectional view); (b) after spin Alq3 (top view); (c) before spin Alq3 (cross-sectional view); and (d) before spin Alq3 (top view).

FIG. 3. (Color online) The room temperature *I-V* curves in the dc bias mode of the ZnO nanoparticle/PF EL device (a) with Alq3; (b) without Alq3.

in nanoparticle aggregations. The pinhole defects could cause the excitons quenching and inconsistent device performance.[15,16] In order to reduce the density of pinhole defects in ZnO nanoparticles, the development of the ZnO nanoparticle monolayer layer is required.

In this study we show that with the dry-coating technique, ZnO nanoparticle monolayer can be achieved in ZnO nanoparticle/polymer composite. During the dry-coating process, the ZnO nanoparticles are adsorbed on the host matrix using ZnO nanoparticle smog during dry-coating process. The ZnO nanoparticle smog is making by homemade nanosmog-making machine, as shown schematically in Fig. 1(b). In the dry-coating procedure, the ZnO nanoparticles may aggregate due to the electrostatic force. However, the latter process using the Alq3 solution could cause the aggregated ZnO nanoparticles without direct contact with the host matrix to disintegrate. The remained ZnO nanoparticles adsorbed on the surface of the hole-transporting layer then form a nanoparticle monolayer (90 nm), which is sandwiched between the organic thin films. The bottom host matrix adsorbs the ZnO nanoparticles. The top electron transporting layer, Alq3, serves three important functions. First, electron injection is enhanced. Second, quenching of radiative recombination near the metal interface is avoided. Third, the ZnO nanoparticle monolayer is achieved.

The field-emission scanning electron microscopy (FESEM) is utilized to examine the formation of the ZnO nanoparticle monolayer. With the process using the Alq3 solution, the ZnO nanoparticles will form the ZnO nanoparticle monolayer on the host matrix (P3HT). Figure 2(a) shows the depth profile of ZnO nanoparticle distribution after an Alq3 thin layer was spun on the ZnO nanoparticles. It can be seen that the ZnO nanoparticle layer with a thickness of 90 nm is sandwiched between the P3HT and the Alq3 thin films. Moreover the Alq3 overlayer can be planar with a smooth surface, as shown in Fig. 2(b). In contrast, without the process using the Alq3 solution, the ZnO nanoparticles will not form the ZnO nanoparticle monolayer. It can be seen from the depth profile in Fig. 2(c) that several layers (approximately microns) of the ZnO nanoparticle are covered on the host matrix (P3HT). For the surface morphology in Fig. 2(d),
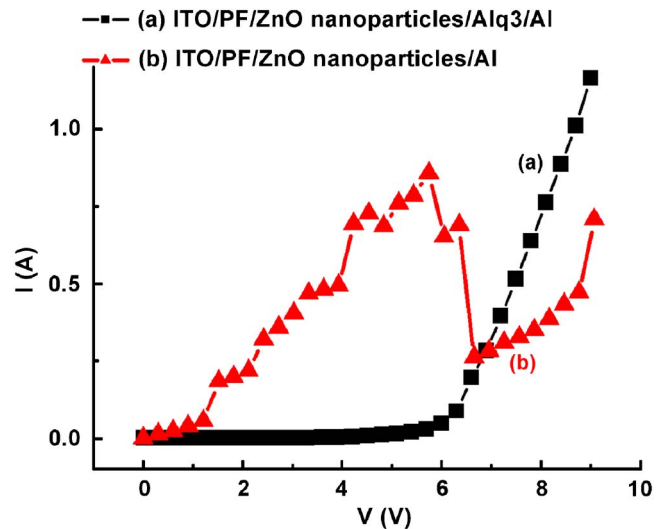
a surface coverage of the ZnO nanoparticle of 89% is obtained. It indicates that the ZnO nanoparticle adsorption on the host matrix during dry-coating process is easy.

The *I-V* curves in dc bias mode of the ZnO EL devices with and without Alq3 are shown in Fig. 3, using Al as the cathode material. For the device with Alq3, the *I-V* curve (curve a) shows stable and good linear *I-V* dependence under forward bias. The turn-on voltage is about 6 V. However, for the device without Alq3, the corresponding *I-V* curve (curve b) is unstable, indicating that the pinhole defects lead to unstable current injection in the ZnO nanoparticles and poor device performance. Hence the electron transporting layer plays a very important role for device performance.

The EL characteristics of the ZnO nanoparticle devices are also measured. Figure 4(a) shows the EL spectra of the three kinds of the ZnO nanoparticle devices under forward bias of 9 V. For the device with PF (device I, curve a), the EL spectrum shows a strong ZnO band-gap emission peak at 380 nm with the broad background emission from PF. The full width at half maximum of the spectrum is 100 nm. For the device with PVK (device II, curve b), it shows a broadband spectrum from 380 to 700 nm, which are the characteristics of the emissions of the ZnO nanoparticles (380 nm) and PVK (553 nm). The emissions indicate that the radiative recombination occurs in the ZnO nanoparticles and at the host matrix/Alq3 interface. For the device with P3HT (device III, curve c) at the same forward bias of 9 V, it also has a peak around 380 nm contributed from ZnO. However the EL spectrum showed another strong background emission peak from P3HT at 655 nm. The suppression of the ZnO band-gap emission and the enhancement of the broad background emission from host matrix imply that the energy transfer from higher-energy emission material (ZnO nanoparticle: 3.3 eV) to lower-energy emission material (P3HT: 1.6 eV) is very strong. Exciton generation on the host matrix occurs via two parallel processes: direct charge injection and exciton transfer from the higher-energy ZnO. For direct charge injection, carriers may be trapped at the host material owing to the voids in the single ZnO monolayer. Alternatively, excitons can be formed in the ZnO nanoparticles that are near the host matrix. These excitons can then undergo Förster energy transfer to the lower-energy host material
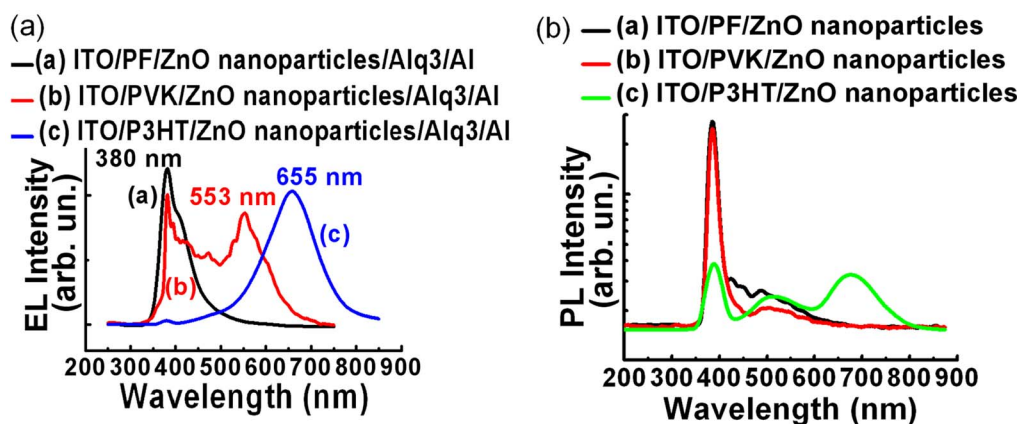
FIG. 4. (Color online) (a) Comparison of EL spectra of ZnO-based nanocomposties with different host matrixes. (b) Room temperature PL spectra of three host matrixes (PF, PVK, and P3HT) with ZnO nanoparticles (The intensities are plotted in logarithmic scale, in order to distinguish from the different intensities of the different samples clearly).

sites, where they recombine radiatively. Thus the enhancement of the ZnO band-gap emission could be addressed by (1) improving the coverage of the ZnO monolayer on the host matrix to increase current injection into the ZnO nanoparticles and (2) using the higher-energy host material to avoid the energy transfer between the ZnO nanoparticles and the host material. In addition, the usual emission around 560 nm from the O-vacancy defects of ZnO is not observed. Also, although Alq3 is used in our devices, its emission around 532 nm does not appear.

To investigate the origin of the EL band, photoluminescence (PL) spectra of host matrix/ ZnO nanoparticles excited using the 266 nm of a Nd-YAG (yttrium aluminum garnet) laser are also measured at room temperature and shown in Fig. 4(b). For the device with the higher-energy host matrix (PF/PVK), the PL spectra show the emission band in the ZnO band-gap emission (380 nm) with a weak emission band from the host matrix. For the device with the lower-energy host matrix (P3HT), the PL spectrum shows the decreased ZnO band-gap emission and the strong host matrix emission, which is due to the Förster energy transfer from the higher-energy ZnO to the lower-energy host matrix. Thus, the ZnO EL device with the lower-energy host matrix causes the poor ZnO band-gap emission.

In conclusion, we report the use of dry-coating technique to fabricate the ZnO nanoparticle EL devices. The dry coating makes the structure of the ZnO nanoparticle monolayer in the device possibly employed. The ZnO monolayer (90 nm) structure can reduce the probability that electrons and holes recombine in the pinhole defects. The FESEM analysis reveals that the ZnO monolayer is sandwiched between the organic transporting materials. Here we demonstrate three types of the ZnO nanoparticle EL devices. These devices show a ZnO band-gap emission peak at 380 nm and

the background emission from the host matrix. The emissions occur via two parallel processes of exciton generation: direct carrier injection and exciton energy transfer. The dry-coating technique revealed in this work shows a convenient way to fabricate ZnO EL devices with very low cost.

[1] C. P. Chen, M. Y. Ke, C. C. Liu, Y. J. Chang, F. H. Yang, and J. J. Huang, Appl. Phys. Lett. **91**, 091107 (2007).
[2] G. Du, Y. Cui, X. Xiaochuan, X. Li, H. Zhu, B. Zhang, Y. Zhang, and Y. Ma, Appl. Phys. Lett. **90**, 243504 (2007).
[3] A. Nakamura, T. Ohashi, K. Yamamoto, J. Ishihara, T. Aoki, J. Temmyo, and H. Gotoh, Appl. Phys. Lett. **90**, 093512 (2007).
[4] S. A. M. Lima, M. R. Davolos, W. G. Quirino, C. Legnani, and M. Cremona, Appl. Phys. Lett. **90**, 023503 (2007).
[5] J. L. Zhao, X. W. Sun, S. T. Tan, G. Q. Lo, D. L. Kwong, and Z. H. Cen, Appl. Phys. Lett. **91**, 263501 (2007).
[6] P. Chen, X. Ma, and D. Yang, Appl. Phys. Lett. **89**, 111112 (2006).
[7] D. J. Rogers, F. Hosseini Teherani, A. Yasan, K. Minder, P. Kung, and M. Razeghi, Appl. Phys. Lett. **88**, 141918 (2006).
[8] W. I. Park and G. C. Yi, Adv. Mater. (Weinheim, Ger.) **16**, 87 (2004).
[9] R. Könenkamp, R. C. Word, and M. Godinez, Nano Lett. **5**, 2005 (2005).
[10] J. Bao, M. Zimmler, F. Capasso, X. Wang, and Z. F. Ren, Nano Lett. **6**, 1719 (2006).
[11] S. J. An and G. C. Yi, Appl. Phys. Lett. **91**, 123109 (2007).
[12] C. Y. Chang, F. C. Tsao, C. J. Pan, G. C. Chi, H. T. Wang, J. J. Chen, F. Ren, D. P. Norton, S. J. Pearton, K. H. Chen, and L. C. Chen, Appl. Phys. Lett. **88**, 173503 (2006).
[13] R. Konenkamp, Robert C. Word, and C. Schlegel, Appl. Phys. Lett. **85**, 6004 (2004).
[14] M. C. Jeong, B. Y. Oh, M. H. Ham, and J. M. Myoung, Appl. Phys. Lett. **88**, 202105 (2006).
[15] E. S. P. Leong and S. F. Yu, Adv. Mater. (Weinheim, Ger.) **18**, 1685 (2006).
[16] C. Y. Lee, Y. T. Huang, W. F. Su, and C. F. Lin, Appl. Phys. Lett. **89**, 231116 (2006).